International Journal of Applied and Advanced Scientific Research (IJAASR)
Impact Factor: 5.255, ISSN (Online): 2456 - 3080
(www.dvpublication.com) Volume 1, Issue 2, 2016

A STUDY ON $Ln_{1-X}M_XMnO_3(0 \leq X \leq 0.5)$(Ln= La, Pr, M= Ba, Ca)CATHODE MATERIAL USED IN IT-SOFCs

P. Matheswaran* & M. Rajasekhar**
* Department of Chemistry, Government Arts College (A), Salem, Tamilnadu
** PG & Research Department of Chemistry, Government Arts College, Dharmapuri, Tamilnadu

Cite This Article: P. Matheswaran & M. Rajasekhar, "A Study on Ln1-XMXMnO3(0 ≤ X ≤ 0.5)(Ln= La, Pr, M= Ba, Ca)Cathode Material Used in IT-SOFCs", International Journal of Applied and Advanced Scientific Research, Volume 1, Issue 2, Page Number 104-108, 2016

Abstract:
This work investigate the effect of synthesis parameters on the crystal structure, electrical conductivity and morphology studies in the intermediate temperature solid oxide fuel cells (IT-SOFCs) of $Ln_{1-X}M_XMnO_3(0 \leq x \leq 0.5)$ perovskite oxides. The lattice parameters were determined at room temperature by X- ray powder diffraction. The lattice volume increases with increasing 'x'. The as-prepared powder was confirmed by XRD studies. The nano particle size was confirmed by x- ray line broadening analysis using the Scherrer equation. The electrical conductivity can be described by small polaron hopping conductivity model. This process remarkably reduced the synthesis time and temperature. The synthesized material showed reasonable electrical conductivity which measured by dc four probe technique.

Key Words: Cathode Material, IT-SOFC, Electrical Conductivity & Rare Earth Manganite

1. Introduction:

Solid oxide fuel cell is an energy conversion device that produces electrical and heat by electrochemical combustion of a fuel with an oxidant [1]. Its major advantages are high efficiency potential for cogeneration, modular construction and very low pollutant emissions. However, its high operation temperature limits the choice of proper materials and decreases the durability. Now the challenge is to develop materials with good performance at intermediate temperatures (600-800° C) for SOFCs allowing it to reduce the cost of the cells, increasing the long term stability and decreasing the time of startup and end. The incorporation of a solid electrolyte has the additional advantage that many problems associated with liquid electrolytes such as corrosion, flooding or electrode distribution may be overcome [2]. A major issue with the reduced operating temperature is the decrease in the catalytic activity of the cathode for oxygen reduction. Although the $La_{1-x}Sr_xMnO_3$perovskite oxide exhibits acceptable electrochemical activity for oxygen reduction at high temperatures with the zirconia electrolyte, its poor oxide ion conductivity prevents its application for IT-SOFCs [3-5]. These drawbacks can be rectified by the development of alternate cathode materials.

Several synthesis methods have been developed for the preparation of perovskite powders such as solid state reaction, sol-gel process and co-precipitation technique [6-9]. The assisted combustion method is particularly useful in the production of ultrafine ceramic powders with a small average particle size and high porosity. This is a simple method with the advantage of using inexpensive precursors and resulting nano sized homogeneous highly reactive powders [10-11]. In this study, the crystal structure, thermal behavior and electrical conductivity of $Ln_{1-X}M_XMnO_3$(x=0-0.5) were investigated. The effect of Ca content on the properties of this series of oxides is discussed. The chemical compatibility of selected compositions with CGO electrolyte was also examined with the aim of their potential application in SOFCs operating at intermediate temperatures [12].

2. Experimental:

2.1 Synthesis: The cathode material $Ln_{1-X}M_XMnO_3(0 \leq x \leq 0.5)$ nano crystalline powder synthesized by combustion process. The materials used in the synthesis were metal nitrates; $Pr(NO_3)_3$, $Ca(NO_3)_2$, $Mn(NO_3)_2$ and the propellant was aspartic acid with high purity. In the combustion process, the metal nitrates were dissolved in distilled water with fuel in order to form homogeneous solution. The solution was stirred well and then heated at 80ºc in the heating mantle. The combustion process was not completed until all the flammable substances are consumed and the resulting material is a foamy powder substance. This powder substance exhibiting voids and pores formed by escaping gases during combustion reaction. The foamy powder was crushed and was kept in a muffle furnace (EDG 3000 3P) at 650º C for 6 hrs. During combustion, aspartic acid released heat which also initiated the solid state reactions leaving no residue. The assisted combustion reaction method was performed at optimized time to obtained phase pure $Ln_{1-X}M_XMnO_3(0 \leq x \leq 0.5)$ nano crystalline powder (Fig. 1). The ignition time and combustion temperature were measured during the synthesis with a thermo couple (K type) [13]. The stoichiometric amount of propellant was determined by calculation based on the valences of oxidizing and reducing elements as determined by the propellant chemistry [14].

2.2 Characterization: The X-ray powder diffractometer (PXRD) analysis (model: Philips X' Pert MPD) was used to identify the phase purity and structural conformation. The diffraction patterns were obtained at 25º C in the range of $20º \leq 2\theta \leq 80º$. The particle size was calculated from XRD line broadening by using Scherrer equation. Thermo gravimetric analysis (TGA) and differential thermal analysis (DTA) of the as prepared

powders were carried out using a TA thermal analyzer (SDT Q600 model) with heating rate of 5°C min^{-1} from room temperature to 1000° C in air [15].

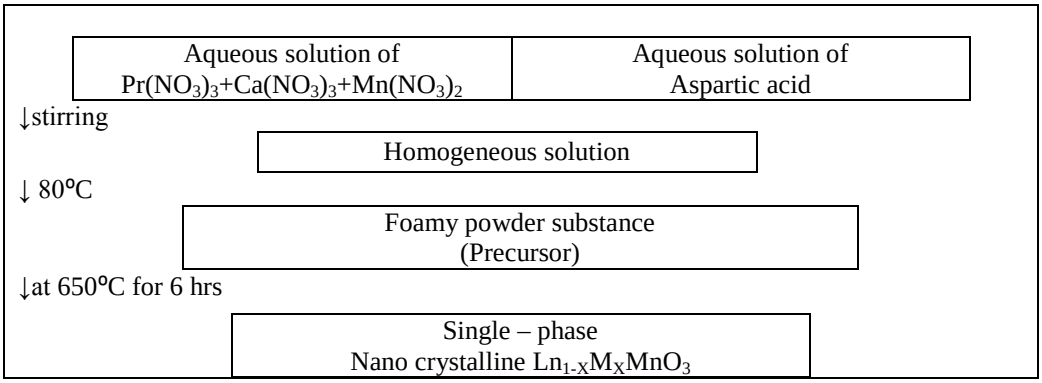

Figure 1: Flow diagram of assisted combustion synthesis of $Ln_{1-X}M_XMnO_3$

The micro structure of praseodymium strontium manganite powder was investigated by scanning electron microscopy (SEM) using Hitachi TM-1000 equipment. Acceleration voltage was 15 kV using backscattering electron [16]. The electrical conductivity of the sintered pellets were measured by a dc-four probe method in the range 200-700°C [17].

3. Results and Discussion:

3.1 Particle Size Analysis: The x-ray diffraction pattern of $Ln_{1-X}M_XMnO_3(0 \leq x \leq 0.5)$ samples are shown in fig. 2. All the samples are single phase materials and the patterns were indexed on the basis of the orthorhombic perovskite structure (space group: Pbnm). The sample calcined at 650°C for 6hrs exhibits a single phase without any impurities. The lattice parameters and the average crystallite sizes are summarized in Table1. The data indicate that the lattice volume increases with increasing Ca content x. These results strongly suggest that assisted combustion methods requires much lower calcination energy with shorter time duration than solid state reaction method.

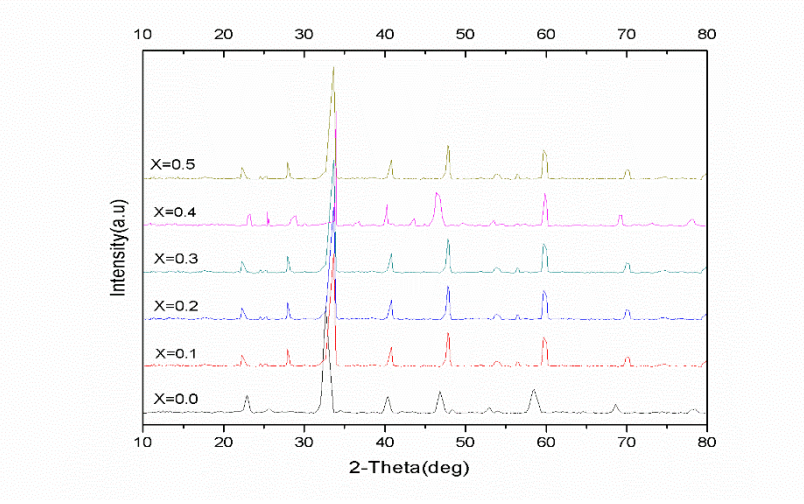

Figure 2: x-ray diffraction pattern of $Ln_{1-X}M_XMnO_3$

The average crystallite size of the sample was calculated using Scherrer equation.

$$D = \frac{0.9\,\lambda}{\beta \cos \theta}$$

Where D is the crystallite size in nm, λ is the radiation wave length (for CuKα radiation,λ =1.54 A°), β is the broadening of the line (half width) in radians and θ is the diffracting peak angle.The average crystallite size values of$Ln_{1-X}M_XMnO_3(0 \leq x \leq 0.5)$ nano powder at various compositions are given in Table 1.The particle size measured from XRD data. The smaller average crystallite size (nano particle) was achieved by using assisted combustion method compared to conventional solid state reaction method.

X(mol)	a (Å)	b (Å)	c (Å)	Lattice Volume ($Å^3$)	Average Crystallite Size (D)	Crystal structure
0.0	6.7218	6.7120	6.7228	303.31	18.76	Ortho Rhombic
0.1	6.7155	6.7265	6.7158	303.36	17.21	Ortho Rhombic
0.2	6.7185	6.7265	6.7197	303.67	19.81	Ortho Rhombic
0.3	6.7166	6.7418	6.7158	304.11	20.66	Ortho Rhombic
0.4	6.7267	6.7269	6.7264	304.37	23.70	Ortho Rhombic
0.5	6.7345	6.7266	6.7346	305.08	19.80	Ortho Rhombic

Table 1: Crystal structure, lattice parameters, lattice volume and average crystallite size of $Ln_{1-X}M_XMnO_3$nano powder

3.2 Thermal Analysis: We have studied the$Ln_{1-X}M_XMnO_3(0 \leq x \leq 0.5)$ nano powder before calcination with thermo gravimetric analysis (TGA) in air as shown in Fig.3a. The profile has shown that thermal decomposition is only complete at 650-750ºC. The first decomposition stage at 150ºC, can be the loss of adsorbed water, the second stage at about 250-550ºCand can be the decomposition of combustion fuels that was not burnt during the fast combustion reaction and the third stage at 650º c is due to the dissociation of carbonates produced during combustion and starting of the formation of $Ln_{1-X}M_XMnO_3(0 \leq x \leq 0.5)$ phase.

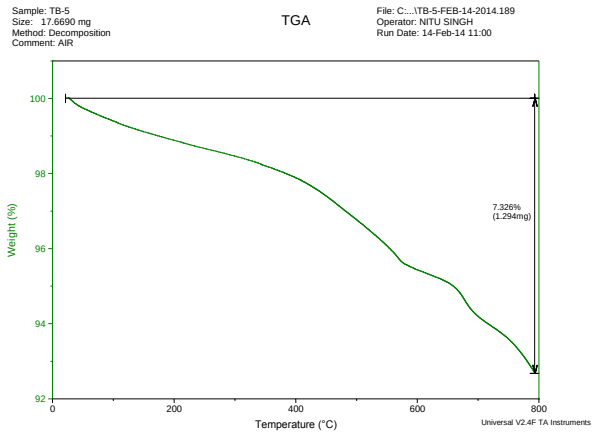

Figure 3a: TGA curve of $Ln_{1-X}M_XMnO_3$nano powder

Figure 3b shows the corresponding DTA curves for the as synthesized powders. For the samples prepared by the combustion method with aspartic acid with more intense peak is observed at 600ºC, which indicate the decomposition of organic residues.DTA curve of the sample prepared with aspartic acid exhibits an intense exothermic peak at 650º C related to the decomposition of aspartic acid not burned during combustion which is characteristic of the oxidation of the propellant [18].

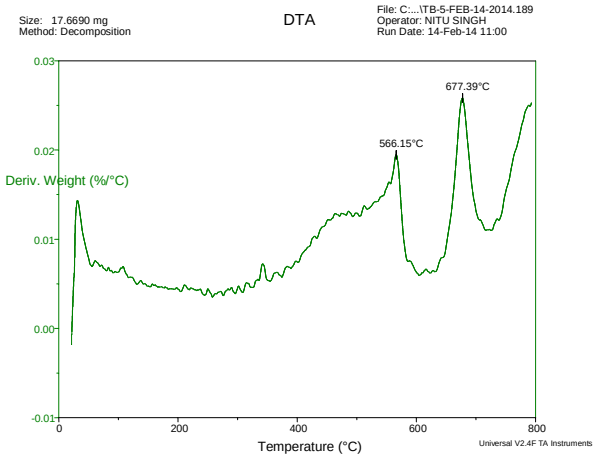

Figure 3b: DTA curve of $Ln_{1-X}M_XMnO_3$nano powder

3.3 SEM Analysis:

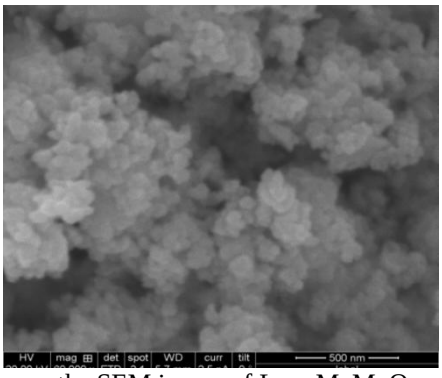

Figure 4: Shows the SEM image of $Ln_{1-X}M_XMnO_3$nano powder

Figure 4 shows SEM analysis of $Ln_{1-X}M_XMnO_3(0 \leq x \leq 0.5)$ nano powder. The materials prepared by combustion method using aspartic acid showed a spongy aspect and the particles were linked together in agglomerates of different sizes and shapes. The loose and porous structure of these materials can be attributed to a significant gas evolution during combustion reaction [19, 20]. Substantial particle growth was observed upon sintering for 6 hrs at 823K. But the structure remained highly porous which resembled the typical cathode structure for SOFC.

3.5 Electrical Conductivity: It can be seen that σ increases with temperature for all the compositions (x =0-0.5). At 650ºC, the electrical conductivity for x = 0.4 is very high. At a given temperature, the conductivity value increases with increasing x due to an increasing Mn^{4+} content and the charge carrier concentration. The charge difference between Pr^{3+} and Ca^{2+} ions is compensated by the formation of Mn^{4+} ions [21]. The electrical conductivity of all the specimen was metallic in behavior and decreased slightly with the elevation of temperature. The high electrical conductivity of$Ln_{1-X}M_XMnO_3(0 \leq x \leq 0.5)$ oxides suggests that the current correction effects are satisfactory when these perovskite oxides are applied for the cathode of SOFC. As a result, Ca doped perovskite oxides prepared in this study are applicable for an oxide cathode of SOFC. The Arrhenius plot of the electrical conductivity (log σ) of $Ln_{1-X}M_XMnO_3$as shown in fig. 5.

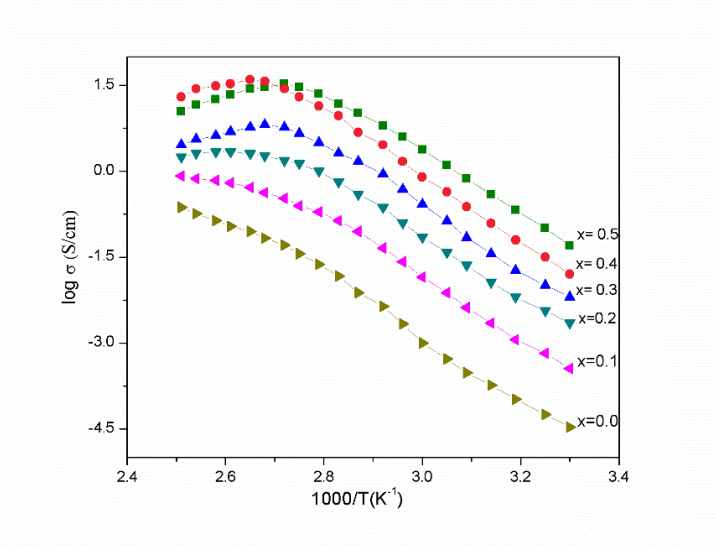

Figure 5: Log σ versus 1000/T for$Ln_{1-X}M_XMnO_3$.

4. Conclusion:

$Ln_{1-X}M_XMnO_3(0 \leq x \leq 0.5)$ perovskite oxides have been evaluated as cathode materials for IT-SOFCs. They have a perovskite type structure with orthorhombic symmetry (Pbnm space group). The electrical conductivity of $Ln_{1-X}M_XMnO_3$is p-type and can be decreased by the small polaron hopping mechanism. The Ca addition is primarily compensated by the formation of Mn^{4+}cations. With increasing Ca content, the conductivity is increased due to the increase in the concentration of Mn^{4+}cations. Among the examined oxides of the system $Ln_{1-X}M_XMnO_3(0 \leq x \leq 0.5)$ the composition with x = 0.4 shows excellent properties required for an intermediate temperature solid oxide fuel cells cathode material by assisted combustion synthesis process and itshigh electrical conductivity value at 650º C is satisfactory for SOFCs.

5. Acknowledgement:

The authors would like to express their gratitude to Prof. A. Subramania, centre for nanoscience and technology, Pondicherry University for helpful discussions and Indian institute of science, Bangalore for the scanning electron microscopy characterization studies.

6. References:

1. Minh, N.Q., J. Am. Ceram. Soc., 1993, 76,563
2. Steele, B. C. H., Phil. Trans. R. Soc. Lond. A. 1996. 354. 1695.
3. T. Horita, K. Yamaji, M. Ishikawa, N. Sakai, H. Yokokawa, T. Kawada and T. Kato, J. Electro chem. Soc., 145, 3196 (1998)
4. F. Zheng and L. R. Pederson, J. Electro chem. Soc, 146, 2810 (1999)
5. R. A. Desouza and J. A. Kilner, Solid State Ionics, 106, 175 (1998)
6. R. J. Bell, G. J. Millar, J. Drennan, Solid State Ionics, 131 (2000) 211-220
7. Q. Zhang, T. Nakagawa, F. Saito, J. Alloys Comp. 308(2000) 121 – 125
8. L. A. Chick, L. R. Pederson, G. D. Maupin, J. L. Bates, L. E. Thomas, G. J. Exarhos, Mater. Lett. 10 (1990) 6-12
9. L. Conceicao, C.R.B. Silva, N.F.P. Ribeiro, M.M.V.M. Souza, Mater. Charact. 60 (2009) 1417-1423.
10. K.C. Patil, S.T. Aruna, T. Mimani, Curr. Opin. Solid State Mater. Sci. 6 (2002) 507 – 512

11. A. VArma, A.S. Rogachev, A.S. Mukasyan, S. Hwang, Adv. Chem. Eng. 24 (1998) 79 – 226
12. G. Ch. Kostogloudis and Ch. Ftikos, J. Euro. Ceramic Soc. 19 (1999) 497 – 505
13. L. Conceicao, Amanda M. Silva, N.F.P. Ribeiro, M.M.V.M. Souza, Mater. Research Bulletin, 46 (2011) 308-314.
14. A. Ringucde, J. A. Labrincha, J. R. Frade, Solid State Ionics 141 – 142 (2001) 549 – 557.
15. L. Conceicao, Amanda M. Silva, N.F.P. Ribeiro, M.M.V.M. Souza, Mater. Research Bulletin, 46 (2011) 308-314.
16. K.T. Lee and A. Manthiram, J. Electrochem. Soc., 152 (1), A 197-A 204 (2005).
17. E. A. Lee, S. Lee, H. J. Hwang, J. W. Moon, J. Power Sources 157 (2006) 709 – 713.
18. M. Biswas, J. Alloys Compd. 480(2009) 942-946.
19. N.P. Bansal, Z. Zhong, J. Power Sources 158(2006) 148-153.
20. D. Berger, C. Matei, F. Papa, D. Macovei, V. Fruth, J. P. Deloume, J. Euro. Ceram. Soc. 27(2007) 4395-4398.
21. G. Ch. Kostogloudis, N. Vasilakos& Ch. Ftikos, J. Euro. Ceram. Soc. 17(1997), 1513 -1521.